Generation of anomalously energetic suprathermal electrons due to collisionless interaction of an electron beam with a nonuniform plasma

I.D. Kaganovich, A.V. Khrabrov, J. Carlsson, Y. Raitses[(a)], D. Sydorenko[(b)], P. Ventzek, L. Chen[(c)],

[(a)]Princeton Plasma Physics Laboratory, NJ
[(b)]University of Alberta, Edmonton, Canada
[(c)]Tokyo Electron America, Austin, TX

Presented to Theory Department on February 4th, 2016
Invited Talk at 2016 DPP by **D. Sydorenko**

PPPL PRINCETON PLASMA PHYSICS LABORATORY

UNIVERSITY OF ALBERTA

TOKYO ELECTRON

OUTLINE

- **Motivation**
- **Brief Summary of Research in Low Temperature Plasma Physics at PPPL**
- **Description of Codes**
- **Beam-plasma interaction in a bounded plasma (two-stream instability):**
  - **Effects of finite size and boundaries**
  - **Effects of nonuniform plasma**
  - **Mechanism of electron acceleration in plasma wave**

PPPL
PRINCETON
PLASMA PHYSICS
LABORATORY

OUTLINE

- **Motivation**

PRINCETON
PLASMA PHYSICS
LABORATORY

FROM METHODS TO CONTROL ELECTRON VELOCITY DISTRIBTUION FUNCTIONS TO PRACTICAL APPLICATIONS

METHODS OF CONTROL

- **Auxiliary biased electrodes**
- **Emission from the surface**
- **Hybrid DC/RF unmagnetized**
- **Magnetized plasma sources**
- **Injection of electron beam into the plasma**

APPLICATIONS

- **Non-ambipolar electron plasma.**
- **DC/RF Plasma Source for Plasma Processing**
- **Tokamak-wall cleaning**
- **Electric Propulsion**
- **High power plasma switch for electric grid system.**

PPPL
PRINCETON
PLASMA PHYSICS
LABORATORY

CONTROLLING PLASMA PROPERTIES WITH APPLIED MAGNETIC FIELD

Applications: Electric Propulsion, Plasma Sources for Ion Beams, Magnetron Discharges, High Power Plasma Switch

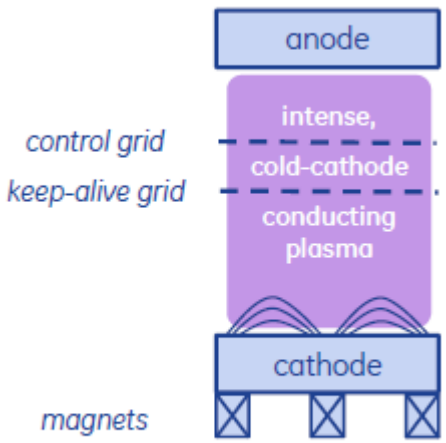

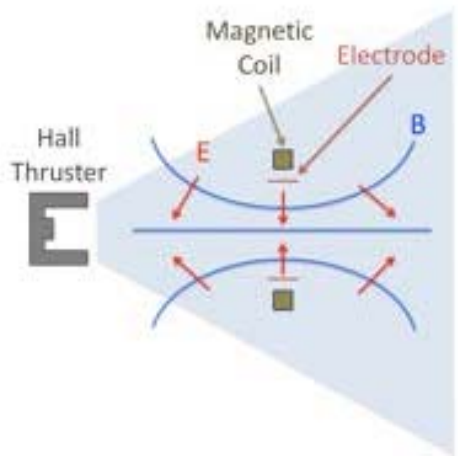

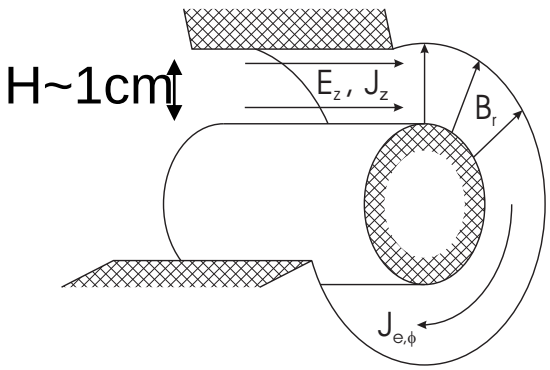

PPPL
PRINCETON
PLASMA PHYSICS
LABORATORY

CONTROLLING PLASMA PROPERTIES BY INEJCTION OF ELECTRON BEAM INTO THE PLASMA

Applications: Plasma Processing Systems, Gas Lasers, Ionization at High Pressures

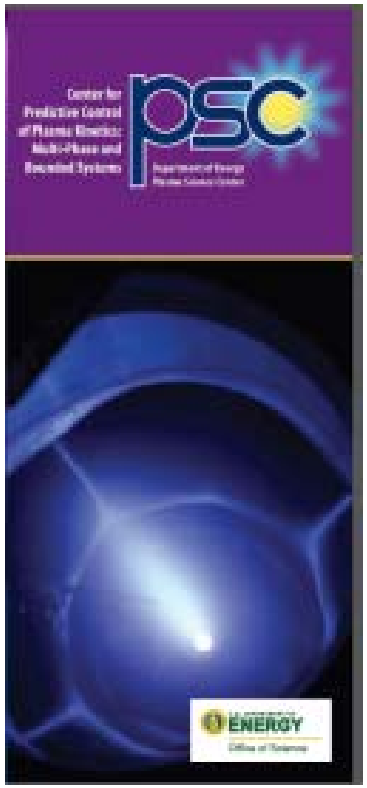

Electron beam generated plasma processing system

Large Area Plasma Processing System (LAPPS)*

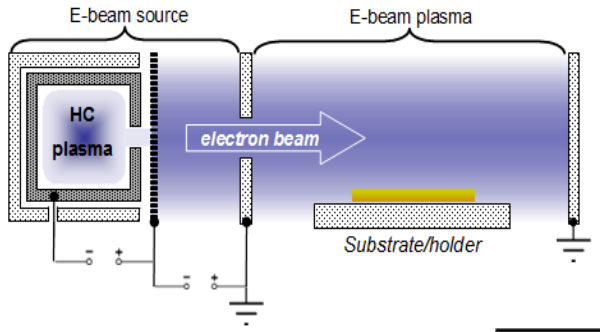

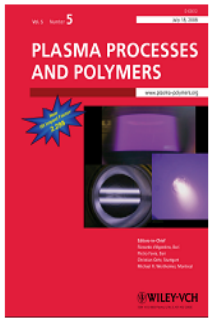

S.G. Walton *et al*, Plasma Proc. and Poly. 5, 453 (2008)

Basic Operation for Processing System

- High-energy (few keV), sheet beam injected into background
- Magnetically collimated to minimize spreading
- Creates plasma sheet parallel to substrate surface
- Large amount of flexibility in system design

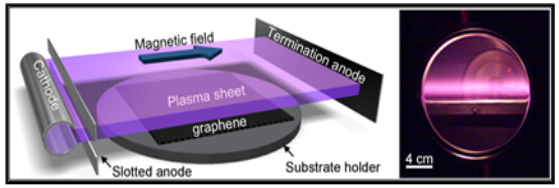

M. Baraket *et al*, App. Phys. Lett. 100, 233123 (2012)

PPPL
PRINCETON PLASMA PHYSICS LABORATORY

* Meger et al., US patent no. 5,874,807 (Feb. 1999)

Revolutionary Nanosynthesis Technologies

Nanomaterials in electronics, energy storage, and environmental and pharmaceutical applications.

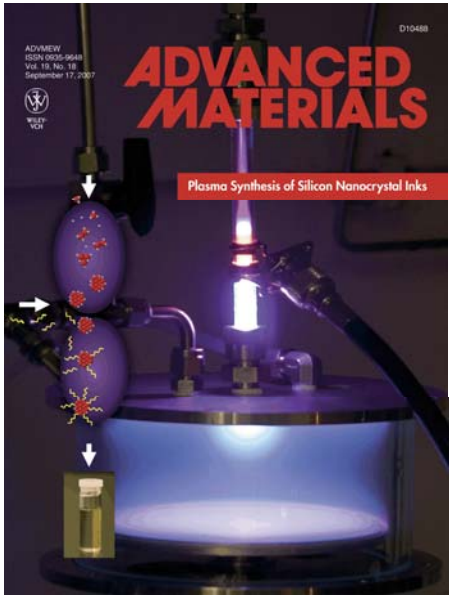

Many existing methods of nanosynthesis use low pressure (10^{-3}-10^{1} torr) and higher pressure ($\leq$ 1 atm.) plasmas to produce a broad range of nanomaterials with various nanostructures:

Low pressure plasma synthesis of silicon nanoparticles.

Mangolini and Kortshagen Advanced Materials 2007 Univ. of Minnesota

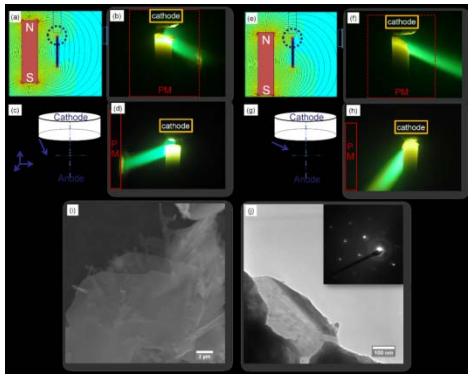

Magnetically controlled arc synthesis of graphene at 500 torr.

Volotskova et al, Nanoscale, 2010 GWU-PPPL-CSIRO

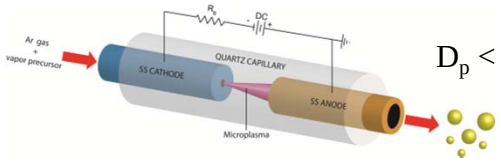

$D_p < 5$ nm

1 atm, room T

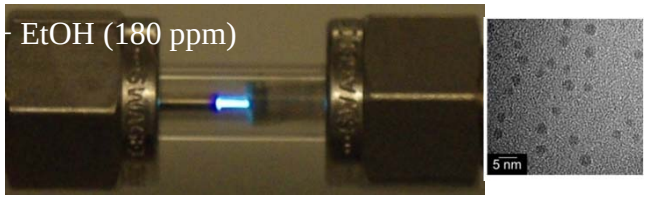

Microplasma synthesis of nano diamonds at 1 atm. pressure

A. Kumar et al., Nature Comm. 2013 Case Western Reserve Univ.

PPPL Plasma Nanotechnology Research

- **Plasma-Based Nanotechnology Laboratory (PBNL) built with internal laboratory support, LDRD, approved by DOE and now fully operational.**

- **PBNL incorporates unique experimental facilities for studies of plasma nanosynthesis and functionalization– leverage from other PPPL PS&T projects supported by DOE FES and DOD.**
- **Initial efforts on modeling of plasma synthesis supported by LDRD.**
- **Collaboration with leading materials science and nanotech experts.**

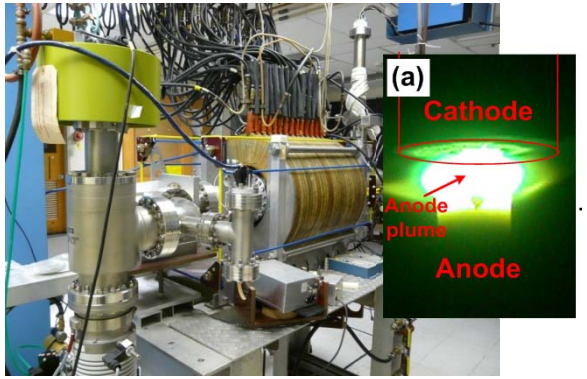

Magnetically Controlled Atmospheric Plasma eXperiment (MAPX) for synthesis of B-C-N nanomaterials.

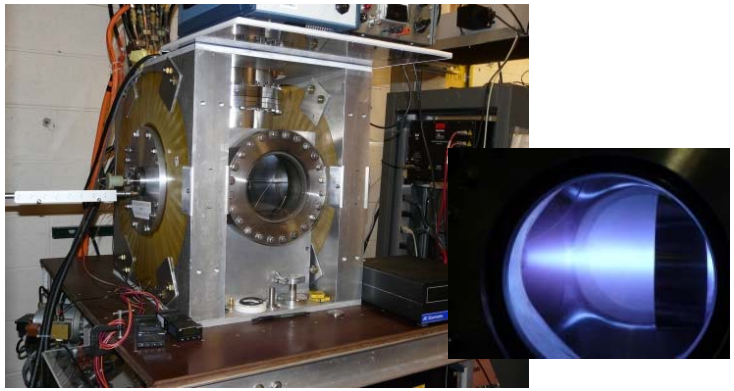

DC-RF plasma-beam system for synthesis, functionalization, and hydrogenation of nanomaterials.

Emerging Plasma-Based Nanotechnologies

Use low-pressure magnetized plasmas to produce new nanomaterials:

Synthesis of nanostructural functional coatings using magnetized plasmas

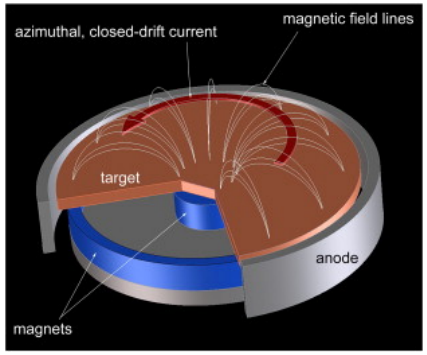

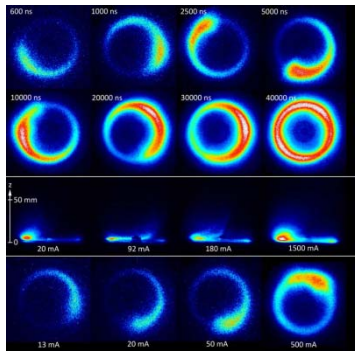

Sputtering magnetron discharge: (a) High power impulse magnetron (HiPIMS); (b) Plasma non-uniformity rotating in E × B direction (DC Magnetron). *A. Anders et al., IEEE TPS to appear in 2014, APL 2013*

Functionalization of nanomaterials by magnetically filtered cold plasmas

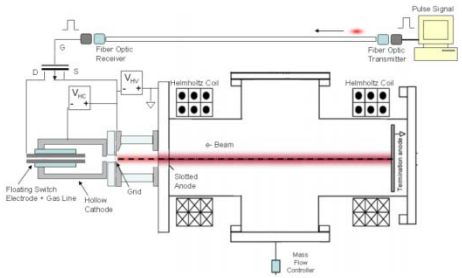

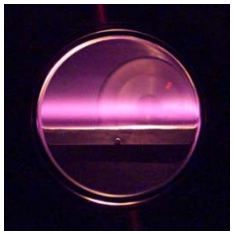

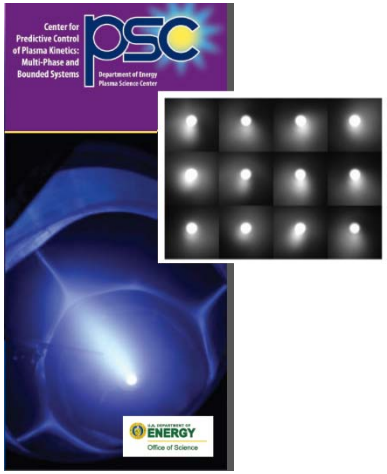

(a) NRL Electron-beam plasma source for functionalization of graphene. *Baraket, Walton et al. 2014*; (b) PPPL DC-RF plasma-beam system and rotating spoke instability. *Raitses et al., DOE PSC meeting 2012*

Need understanding of relevant plasma instabilities and plasma-surface interactions at nanoscale level to control quality of synthesis and functionalization processes and nanomaterials.

RECENT SPECIAL TOPIC JOURNAL SECTIONS DEDICATED TO ELECTRON KINETICS

- **Plasma Sources Science Technology (PSST) 2015. Electron heating in technological plasmas, Guest Editors: Thomas Mussenbrock Julian Schulze**
- **PSST 2014. Spots and patterns on electrodes of gas discharges, Guest Editors: Mikhail S Benilov and Ulrich Kogelschatz**
- **PSST 2014. Interaction of electromagnetic waves with low temperature plasmas, Guest Editors: Osamu Sakai and Shahid Rauf**

- **Workshop at the 65th GEC, 2012, on "Plasma Cross Field Diffusion" =>**

  PSST 2014, Transport in B-fields in Low-Temperature, Rod Boswell and Igor Kaganovich
- **Workshop at the 64th GEC, 2011, "Control of Distribution Functions in Low Temperature Plasmas" organized by, Yevgeny Raitses, David Graves, and Gottlieb Oehrlein => Special Topic, Phys. Plasmas 20 (2013), "Electron kinetic effects in low temperature plasmas", Igor D. Kaganovich, Vladimir Kolobov, Valery Godyak.**

OUTLINE

- **Description of Codes**

PRINCETON
PLASMA PHYSICS
LABORATORY

PARTICLE-IN-CELL CODES ARE USED TO RESOLVE COMPLEX MICRO PHYSICS

An electrostatic parallel, implicit, 1D PIC code EDIPIC. Implemented electron-atom scattering, ionization, and excitation as well as electron-ion and electron-electron collisions, electron induced emission.

3D LSP code also includes electromagnetic and electrostatic modules.

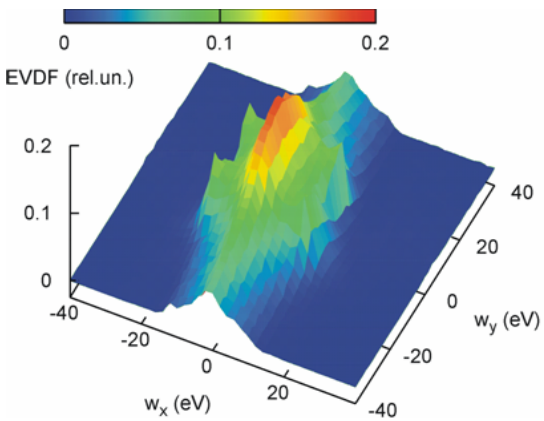

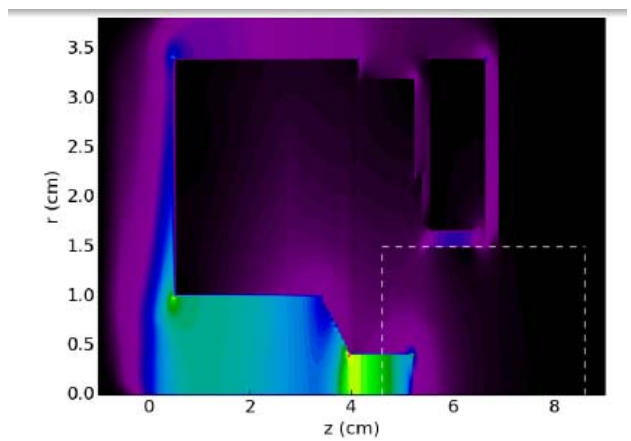

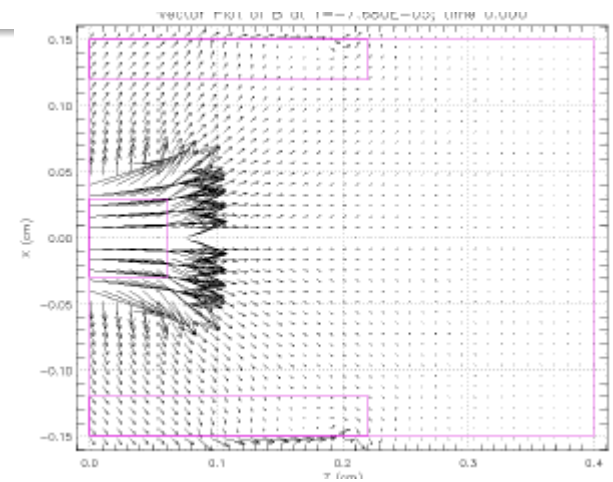

D. Sydorenko, *et al*, Phys Rev Lett., 103 145004 (2009).

IMPROVEMENTS IN LSP CODE

- **LSP code 3D - Electrostatic and Electromagnetic Particle-In-Cell code includes:**
  - **Implicit, Explicit Electrostatic and Electromagnetic solvers**
  - **Full collision algorithm for isotropic elastic and inelastic collisions.**
- **Improvements:**
  - **New Electrostatic PETSc Solvers**
  - **Anisotropic elastic and inelastic collisions**
  - **External circuit**

BENCHMARKING OF CODES

E. A. Den Hartog, D. A. Doughty, and J. E. Lawler, ”Laser optogalvanic and fluorescence studies of the cathode region of a glow discharge”, Phys. Rev. A 38, 2471 (1988).

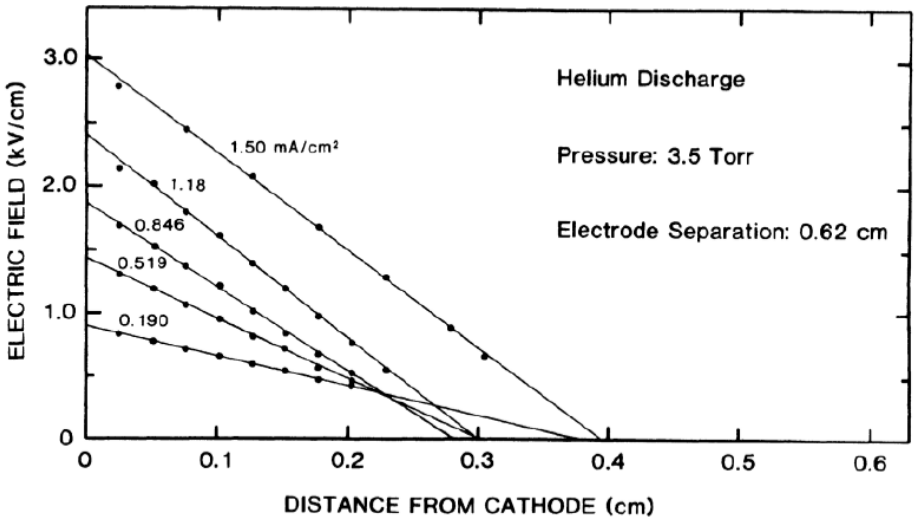

Accurate and complete measurements of the plasma quantities: E(x), γ, J, U.

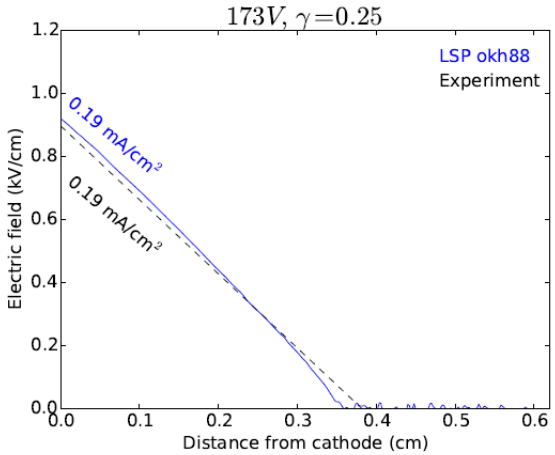

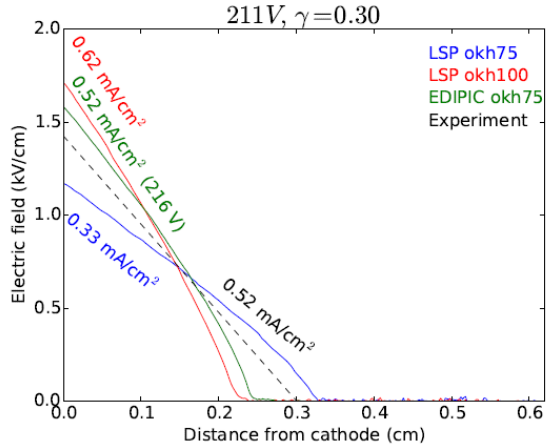

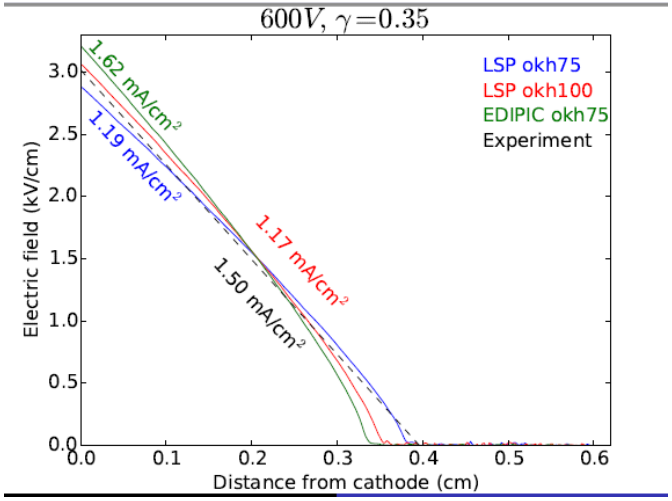

OUTLINE

- **Very brief summary of results on effects of emission**

CONTROLLING PLASMA PROPERTIES: ELECTRON INDUCED SECONDARY ELECTRON EMISSION

- **Kinetic studies of bounded plasmas by walls having secondary electron emission (SEE) predict a strong dependence of wall potential on SEE [1-4].**
- **Sheath oscillations occur due to coupling of the sheath potential and non-Maxwellian electron energy distribution functions [1,2].**

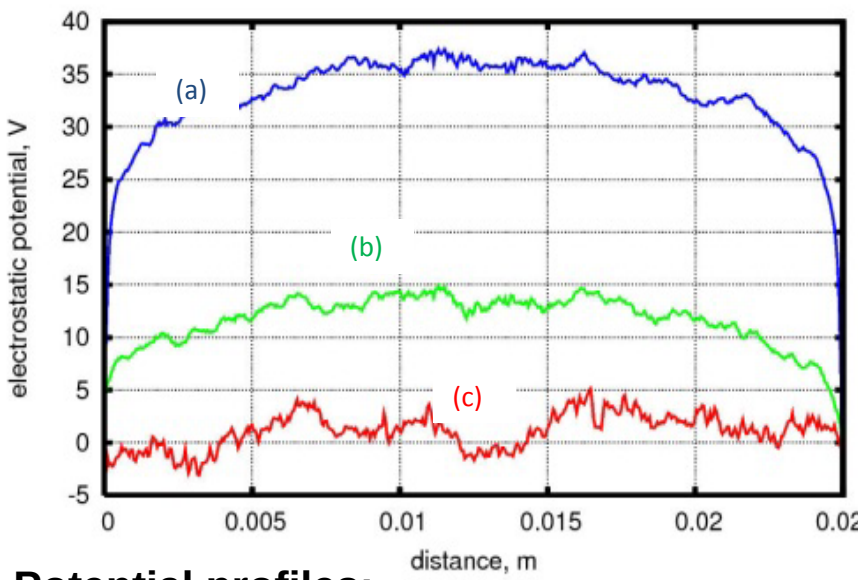

Potential profiles:
(a) E=200V/cm no emission
(b) E=200V/cm with SEE,
(c) E =250V/cm with SEE [1,3]

- **When electrons impacting walls produce more than one secondary on average no classical sheath exists.**
- **Strong dependence of wall potential on SEE allows for active control of plasma properties by judicious choice of the wall material.**

[1] Phys. Rev. Lett. 103, 145004 (2009)
[2] Phys. Rev. Lett. 108, 235001 (2012)
[3] Phys. Rev. Lett. 108, 255001 (2012)
[4] Phys. Plasmas 19, 123513 (2012)

PPPL PRINCETON PLASMA PHYSICS LABORATORY

UNIVERSITY OF ALBERTA

PLASMA POTENTIAL NEAR EMITTING SURFACE IN COMPLEX PLASMAS

JP Sheehan measured sheath potential between emitting wall and plasma and showed that it vanishes as plasma temperature approaches temperature of the emitted electrons. J. P. Sheehan et al, PoP (2014); PRL (2013).

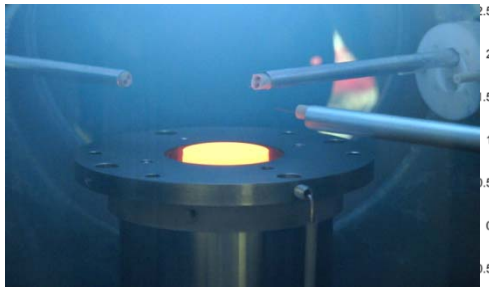

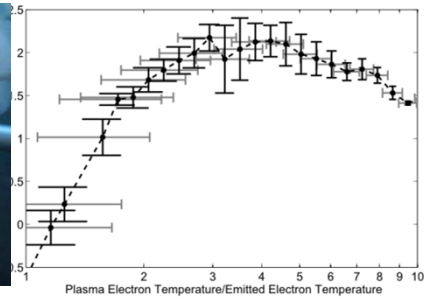

X. Wang, J. Pilewskie, H.-W. Hsu, and M. Horányi measured sheath potential between emitting wall and plasma and showed when the emitted electron density becomes larger than the plasma electron density, a monotonic inverse sheath forms with a positive surface potential relative to the ambient.

Geophys. Res. Lett. 10.1002/2015GL067175

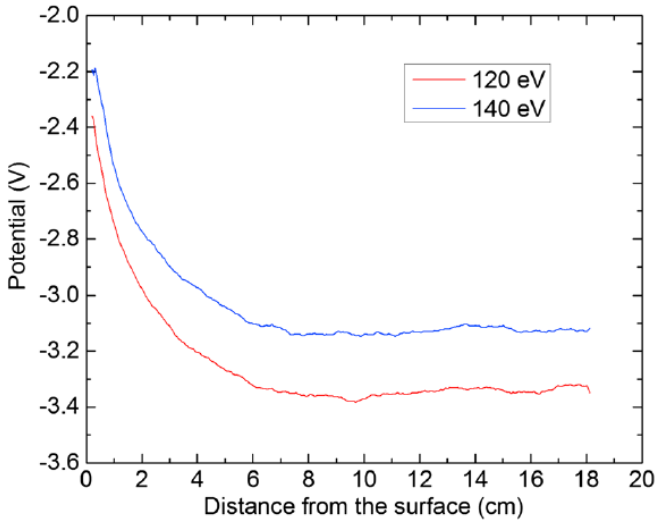

Figure 5. The potential profiles above the surface show the inverse sheaths with E_b of 120 and 140 eV. The chamber is kept under vacuum with the pressure of $P_{Ar} = 6 \cdot 10^{-7}$ Torr.

OUTLINE

- **Beam-plasma interaction in a bounded plasma (two-stream instability):**

PRINCETON
PLASMA PHYSICS
LABORATORY

Etcher with a capacitively coupled plasma and a RF-bias wafer electrode and DC biased electrode

DC biased electrode 800V

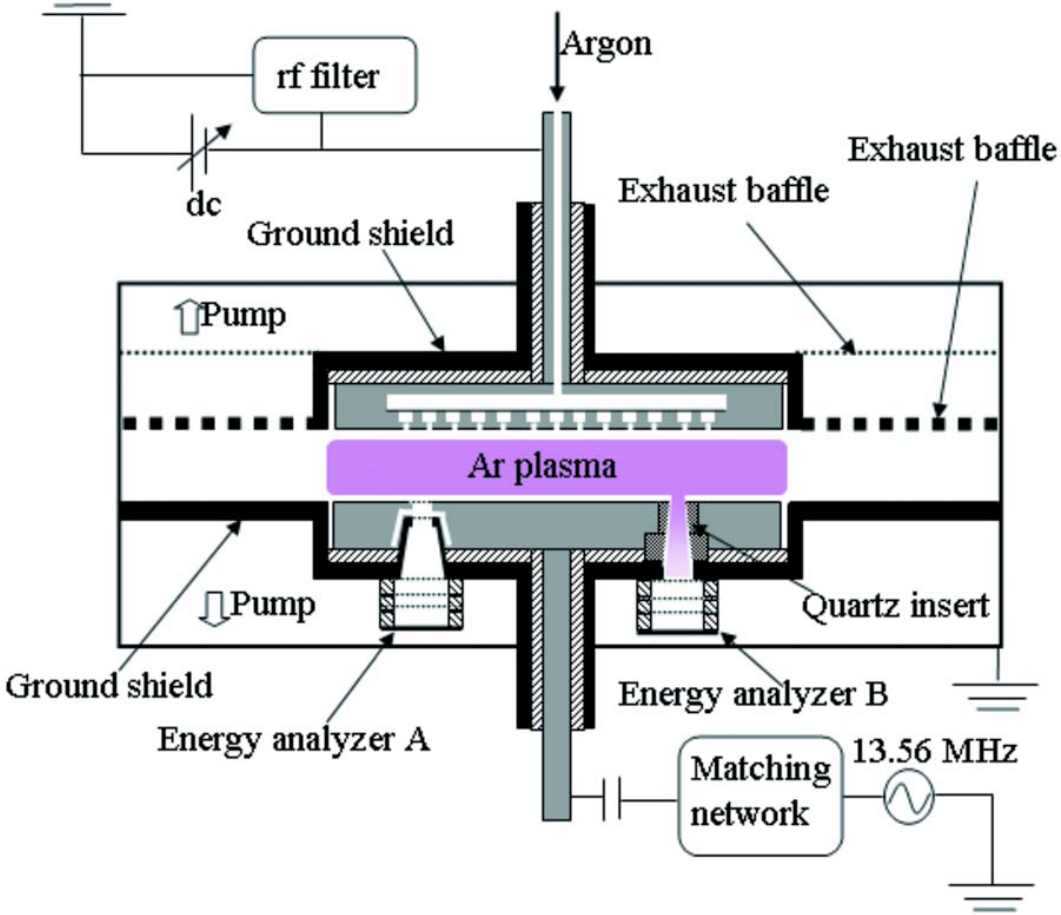

RF biased electrode (1-2kV) with wafer and electron energy analyzers

US Patent 7829469

.

Simplicity and Reliability

- **Wide pressure window**
- **Independent control of the plasma generation and ion energy**
- **Rich in molecular radicals**

Experimental measurements show formation of complex electron energy distribution function

A high energy beam with energy equal to the biased voltage, middle energy peak and low energy bulk electrons in the electron energy distribution function (EEDF) has been observed in a DC/RF discharge. L. Xu et al, Appl. Phys. Lett. 93, 261502 (2008).

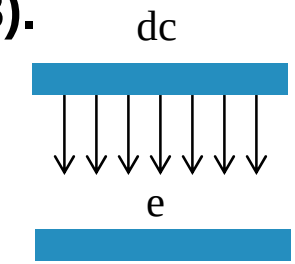

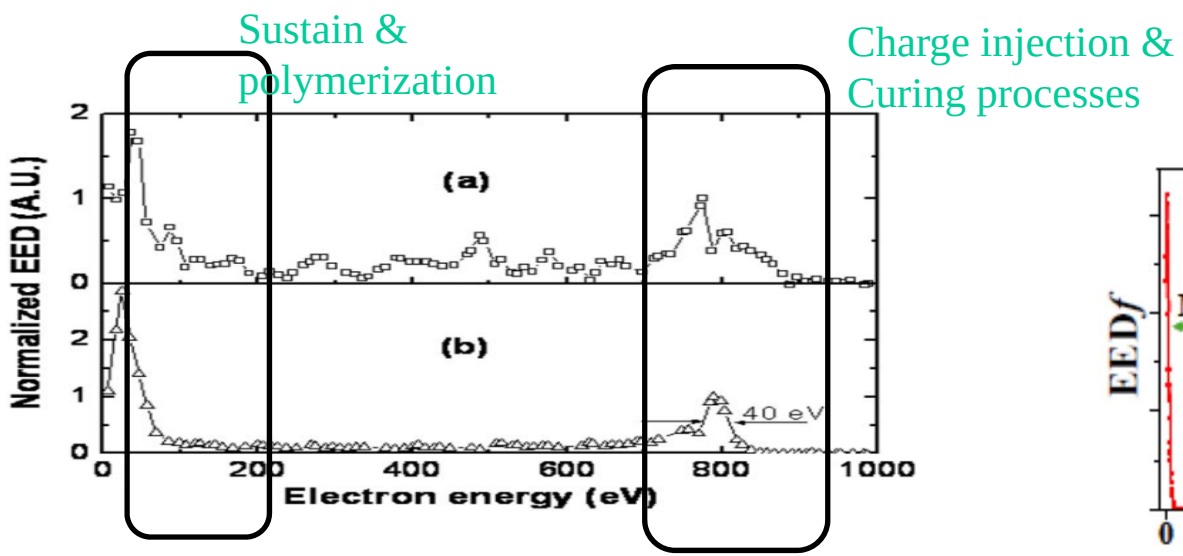

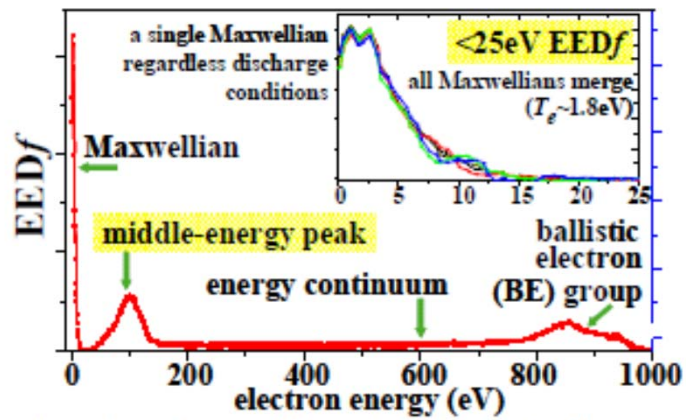

Fig. 1. Non-Maxwellian EED*f* of DC/RF plasma.

COMPLEX ELECTRON ENERGY DISTRIBUTION IN ASYMMETRIC RF-DC DISCHARGE

- An analytical model A. Khrabrov, et al, PSST (2015)

- Schematics of electron trajectories in RF-DC discharge in (t, x) phase space. RF electrode is positioned at the bottom and DC at the top. Red curve shows schematically the position of the RF sheath boundary, the green curve - the position of the DC sheath boundary. The trapping, dumping and single-pass intervals show RF phases with different dynamics for electrons emitted from the DC electrode.

- Plot of energy $E_{RF}(\psi) = V_{RF}(\psi) - V_{RF}(\phi(\psi))$ for electrons originated from the RF electrode at phase ψ and exiting at phase ϕ. Right axis shows number of bounces in the gap performed until exiting to the electrode. The blue envelope is $V_{RF}(\psi) - V_{RF}(\pi)$

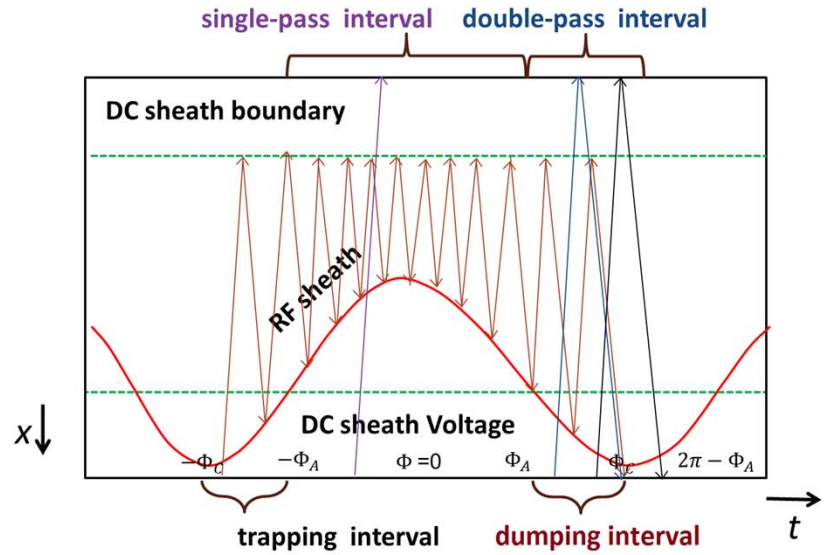

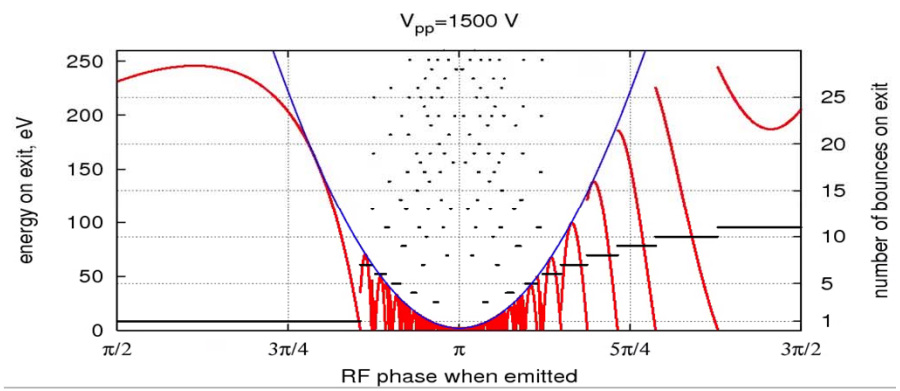

COMPLEX ELECTRON ENERGY DISTRIBUTION IN ASYMMETRIC RF-DC DISCHARGE

- **Low-pressure capacitively-coupled discharges with additional DC bias applied to a separate electrode are important for plasma-assisted etching for semiconductor device manufacturing. Measurements of the electron energy distribution function (EEDF) impinging on the wafer and in the plasma bulk show complex structure of EEDF with multiple peaks and steps.**
- **An analytical model has been developed to predict existence of peaked and step-like structures in the EVDF. These features can be explained by analyzing the kinematics of electron trajectories in the discharge gap.**
- **A. Khrabrov, et al, PSST (2015)**

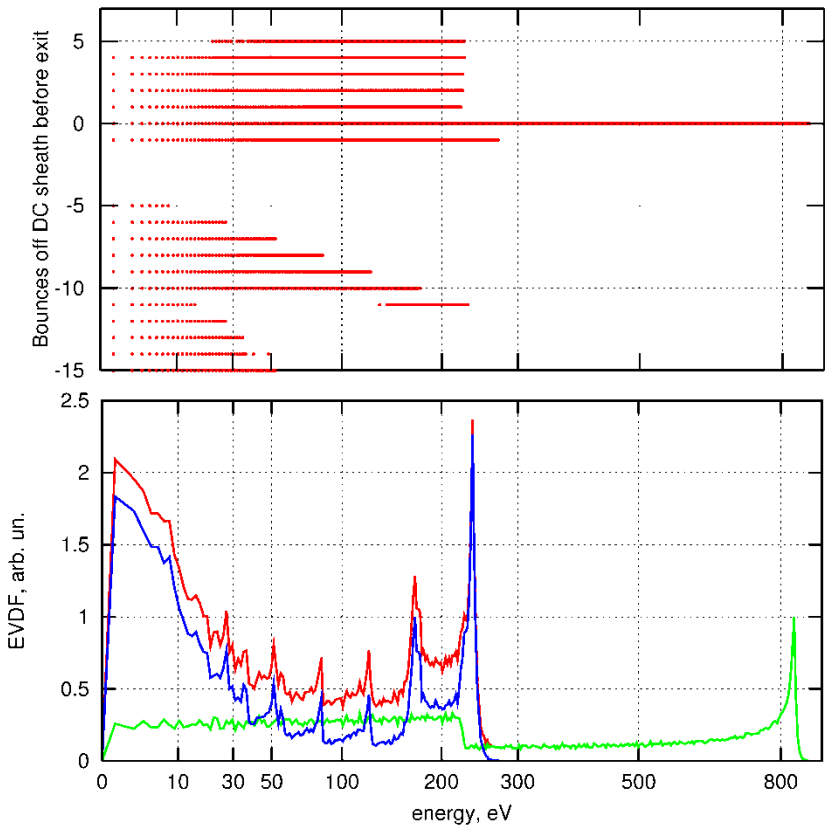

- **Electron Energy Distribution Function showing correlation between number of bounces and energy peaks**

CONTROLLING PLASMA PROPERTIES BY INEJCTION OF ELECTRON BEAM INTO THE PLASMA

Electron beam is self generated in RF/DC system or by injection from the source.
Electron beam emitted from the walls can interact with plasma and effectively transfer energy to background electrons and ions.

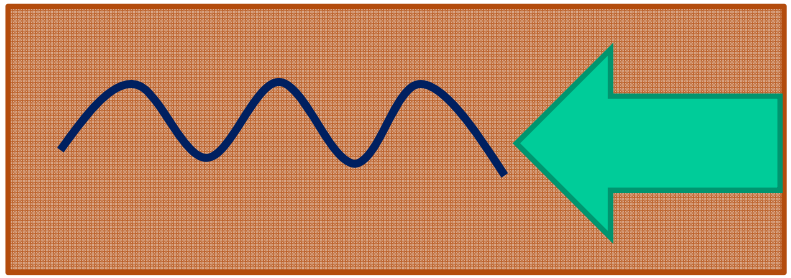

Questions:

How effective is this process?
What are resulting electron and ion energy distribution functions?

Langmuir paradox and Langmuir turbulence revisited.
Still no answer in 3D and for realistic geometry!

PPPL
PRINCETON PLASMA PHYSICS LABORATORY

DC SYSTEM SIMULATED WITH EDIPIC

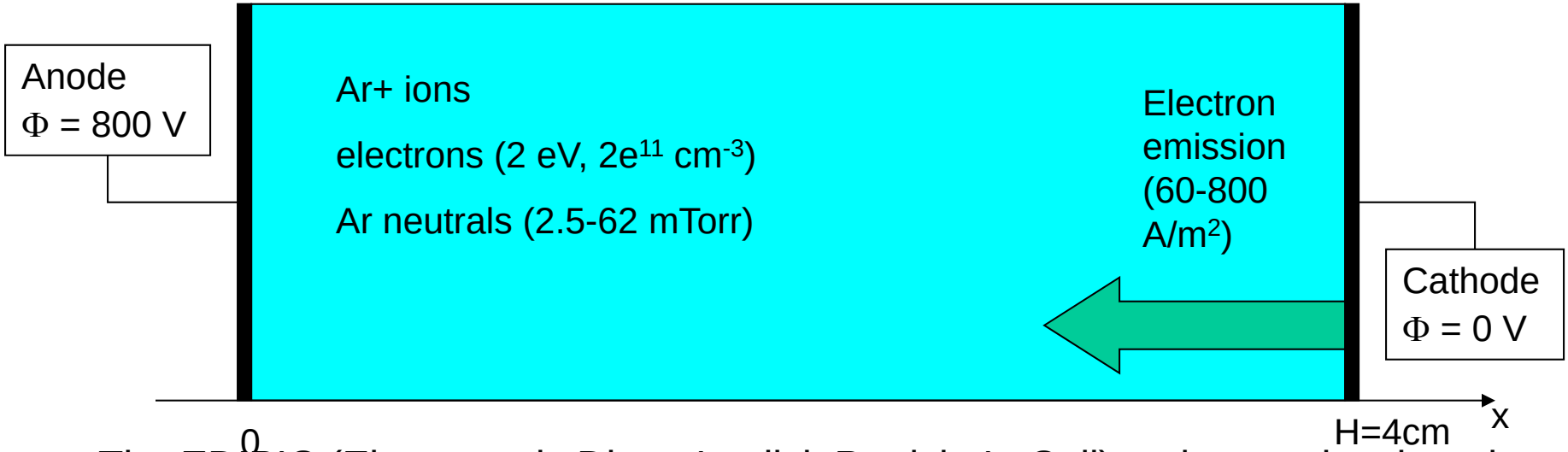

- The EDIPIC (Electrostatic Direct Implicit Particle In Cell) code was developed by D. Sydorenko for simulation of Hall discharges, beam-plasma interaction, plasma sheath.
- EDIPIC code features:
  - Electrostatic, direct implicit algorithm
  - Electron-neutral and Coulomb collisions
  - Secondary electron emission
  - Multiple choices of boundary conditions (emitting/non-emitting walls, plasma source, periodic boundaries)
  - Abundant diagnostics output
  - MPI parallelization

SIMULATION OF MULTI-PEAK ELECTRON VELOCITY DISTRIBUTION FUNCTION

Electron velocity

Ion velocity

Density

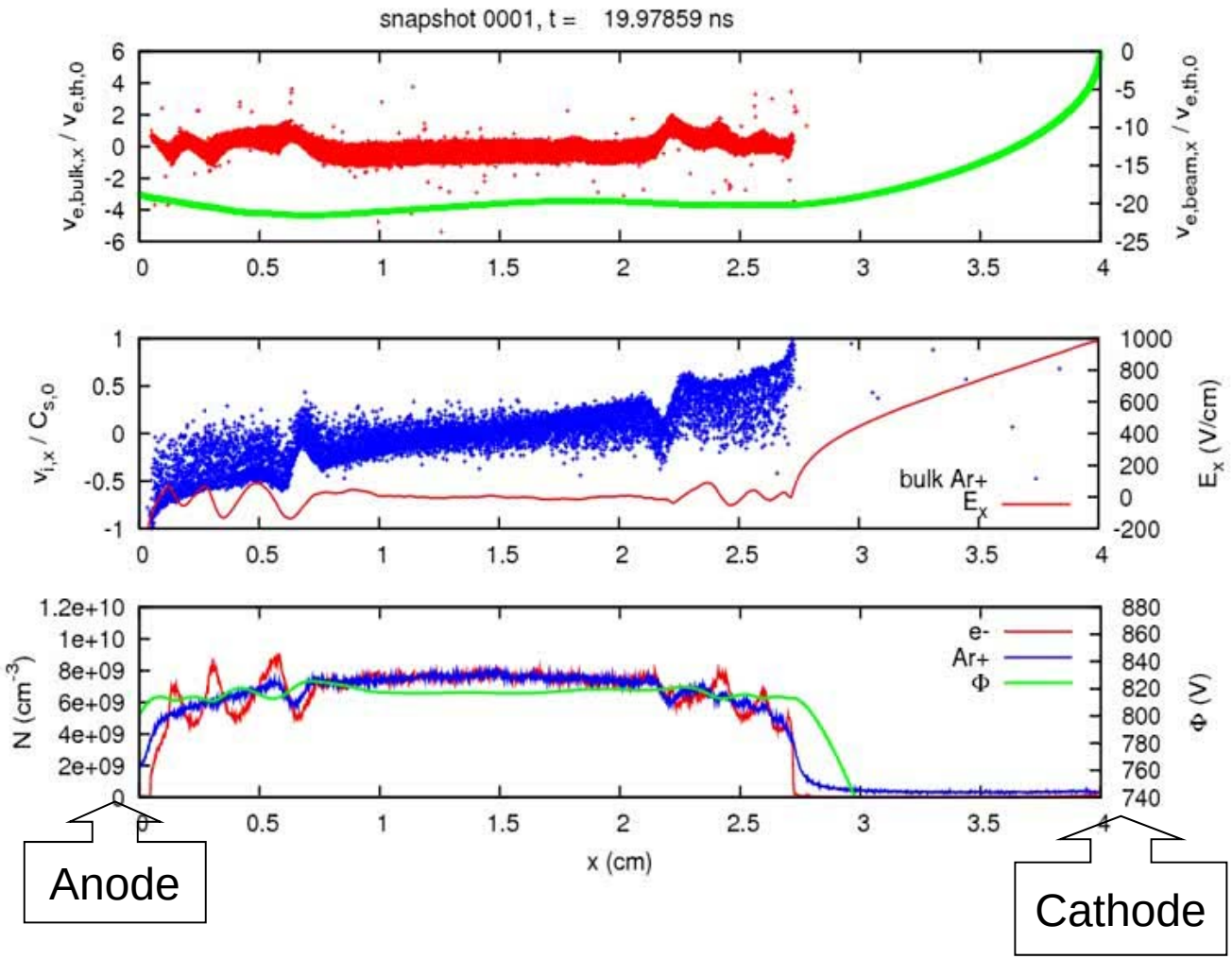

red = bulk

green = beam

Electric field

Electro-static potential

ELECTRIC FIELDS CAN REACH kV/cm WITH BEAM CURRENT OF 20 mA/cm^2

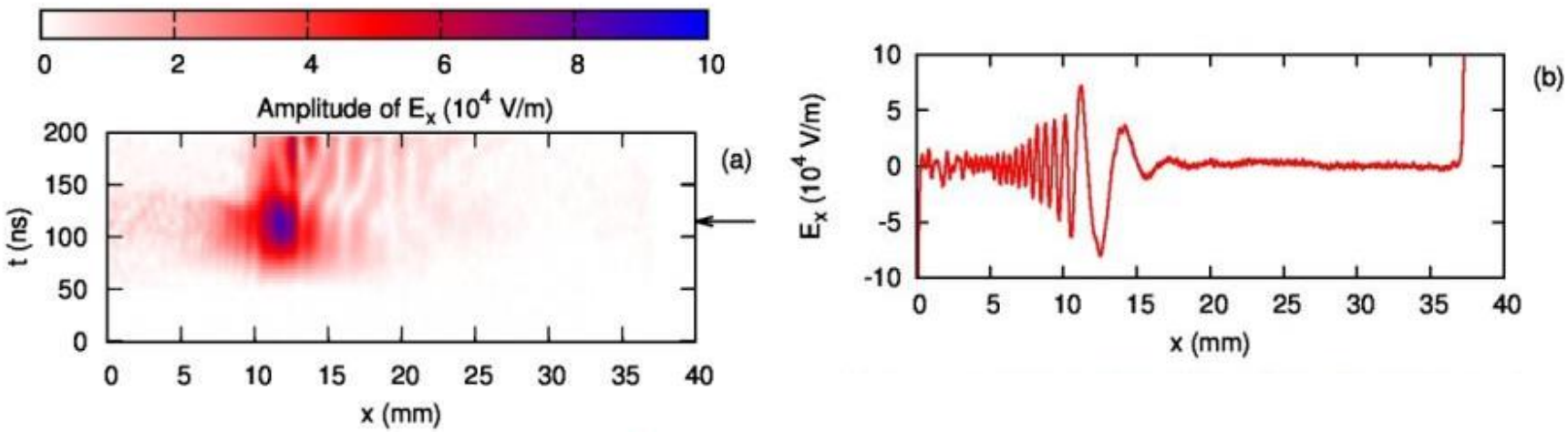

Now there is sufficient "kick" from the electric field to accelerate electrons out of the background.

PPPL PRINCETON PLASMA PHYSICS LABORATORY

UNIVERSITY OF ALBERTA

SIGNIFICANT ACCELERATION OF BULK ELECTRONS

Snapshot 1, lowered frequency regime

Electron bulk (**red**) and beam (**blue**) phase plane

EVDF of bulk (**red**) and beam (**blue**) electrons

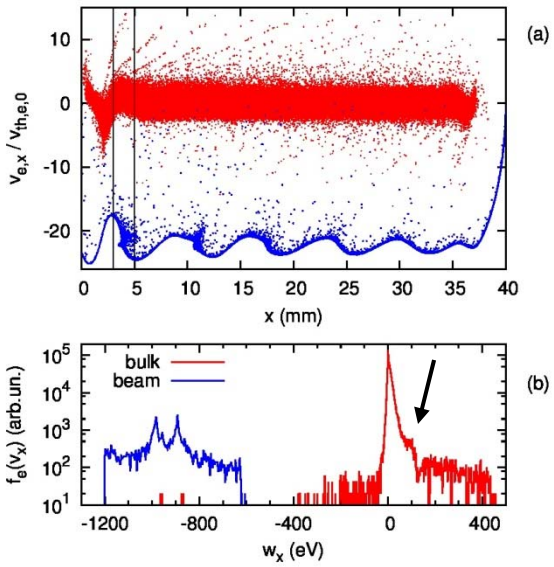

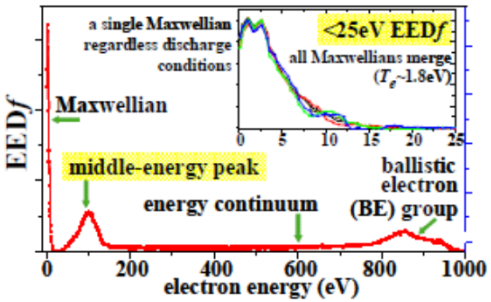

Fig. 1. Non-Maxwellian EEDf of DC/RF plasma.

From [*Chen and Funk*, 2010].

Snapshot 2, ordinary regime

Electron bulk phase plane

Emitted electrons phase plane

EVDF of bulk electrons in area A

EVDF of bulk electrons in area B

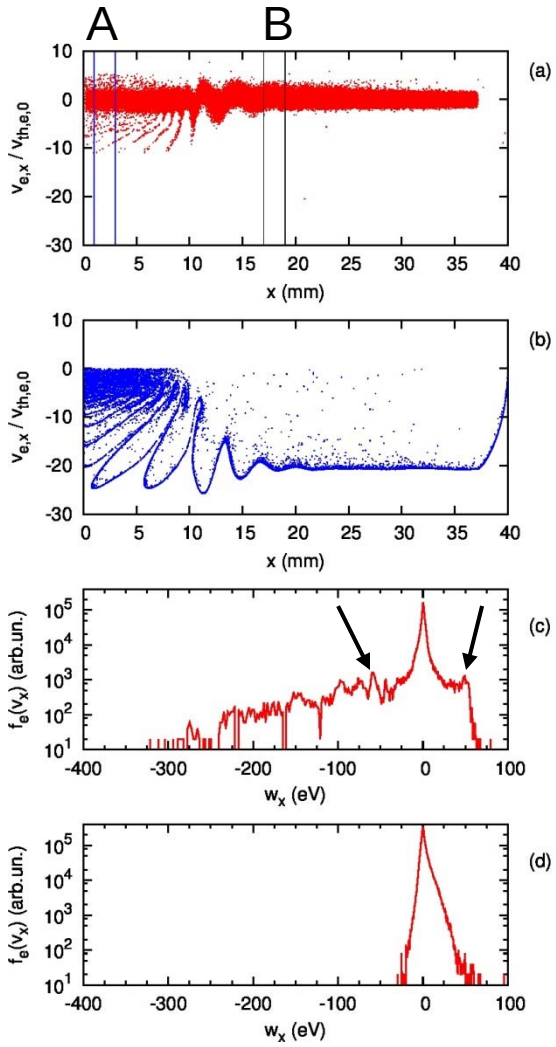

Arrows mark super-thermal electrons

OUTLINE

- **Beam-plasma interaction in a bounded plasma (two-stream instability):**
  - **Effects of finite size and boundaries:**

    We developed analytical theory for threshold of instability as function of plasma parameters and collisions

PRINCETON
PLASMA PHYSICS
LABORATORY

Pierce Model (1944)

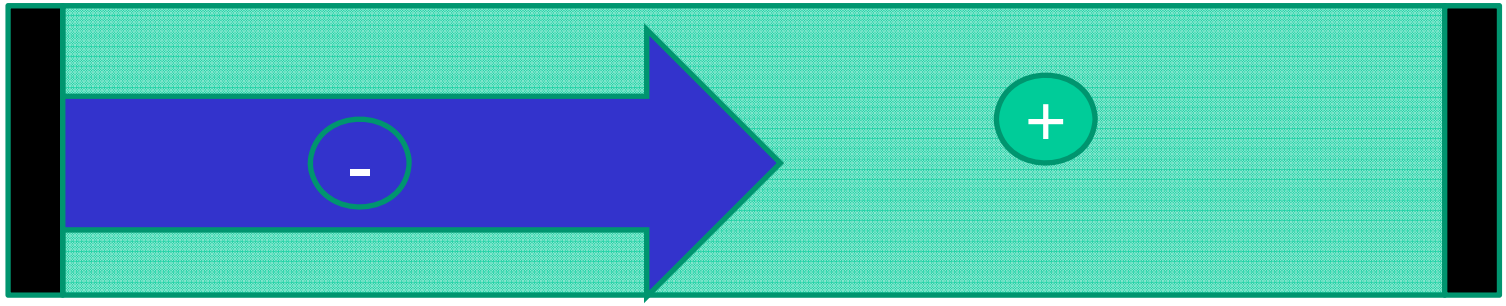

Electron beam is injected into ion background of equal density to the electron beam.

Electrodes with fixed potential set potential at boundaries.

Instability develops if $\omega_{pb} L / v_b > \pi$

This limits the current propagation through the gap.

Our Model (2015?)

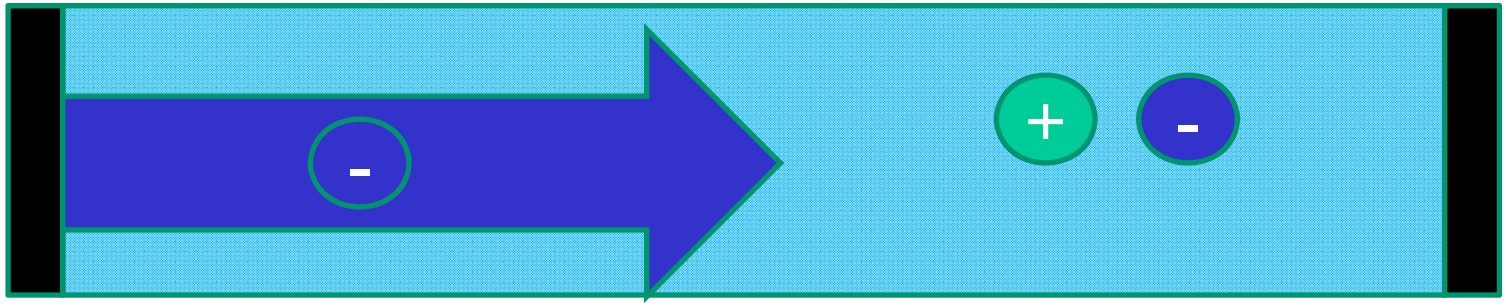

Electron beam is injected into electron and ion background of equal density.

Electrodes with fixed potential set potential at boundaries.

Instability is very different from textbook calculation for periodic b.c. $\omega_{e,0}\left(n_{b,0}/n_{e,0}\right)^{1/3}$

Analytic Solution

$$\frac{\partial n_{e,b}}{\partial t} + \frac{\partial v_{e,b} n_{e,b}}{\partial x} = 0$$

$$\frac{\partial v_{e,b}}{\partial t} + v_{e,b}\frac{\partial v_{e,b}}{\partial x} = -\frac{e}{m}E$$

$$\delta n_b(0) = \delta v_b(0) = \delta\phi(0) = \delta\phi(L) = 0$$

$$\delta\phi(t,x) = \left(Ax + Be^{ik_+x} + Ce^{ik_-x} + D\right)e^{-i\omega t},$$

the following additional relation between ω and k:

$$k_-^2\left(e^{ik_+L} - 1\right) - \frac{ik_-^2 k_+ \omega L}{\omega - k_+ v_{b,0}} = k_+^2\left(e^{ik_-L} - 1\right) - \frac{ik_+^2 k_- \omega L}{\omega - k_- v_{b,0}}.$$

$$k_\pm = (1 \mp \chi)\frac{\omega_{e,0}}{v_{b,0}}$$

(10)

$$-i\frac{2(1-\chi)}{(1+\chi)\chi}L_n + e^{i(1-\chi)L_n} - 1 - \frac{(1-\chi)^2}{(1+\chi)^2}\left[e^{i(1+\chi)L_n} - 1\right] = 0$$

BANDWIDTH STRUCTURE OF GROWTH RATE OF TWO-STREAM INSTABILITY OF AN ELECTRON BEAM PROPAGATING IN A BOUNDED PLASMA

- **An analytical model of two-stream instability development,**
- **I. Kaganovich and D. Sydorenko (2015)**

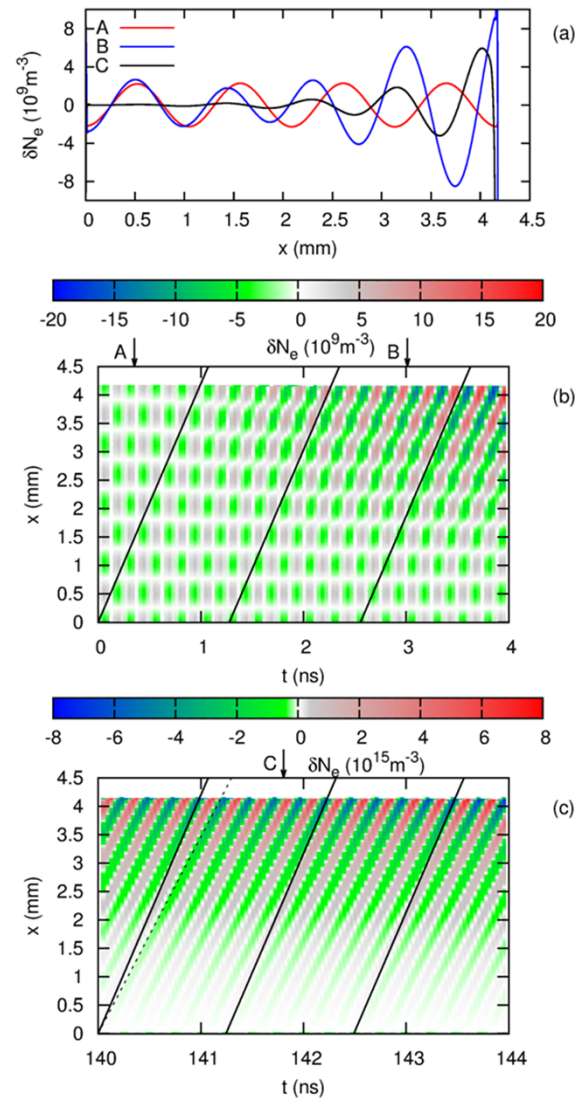

Fig. Dynamics of two-stream instability, the beam to plasma density ration, = 0.0006.
(a) Spatial profiles of bulk electron density perturbation obtained at t=0.35ns (curve A, red), t=3.01ns (curve B, blue), and t =141.8ns (curve C, black).
Panels (b) and (c) are color maps of evolution of density perturbations of bulk electron density in time intervals (b) 1-4ns, (c) 140-144ns. Here, solid black straight lines represent propagation with unperturbed beam velocity; dashed straight line represents phase velocity of the wave.

Comparison of analytic theory and PIC simulations

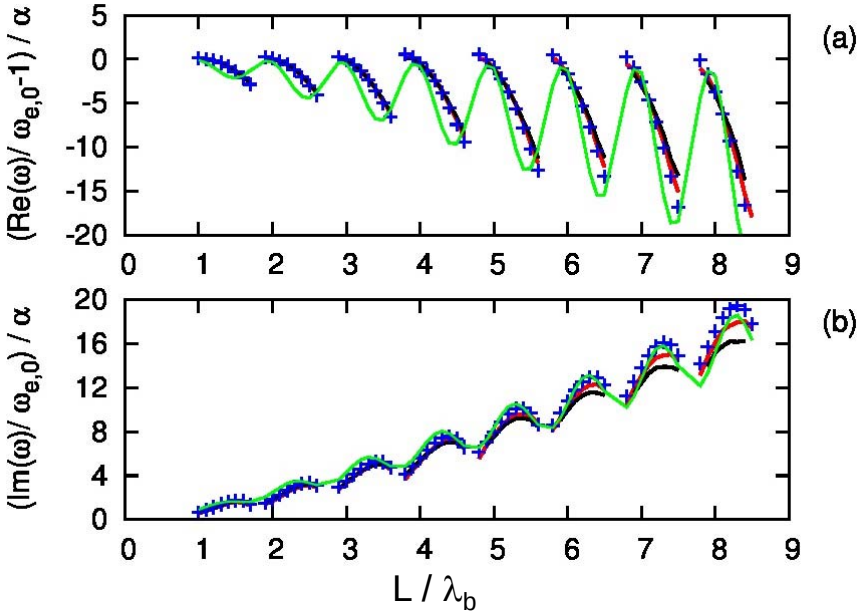

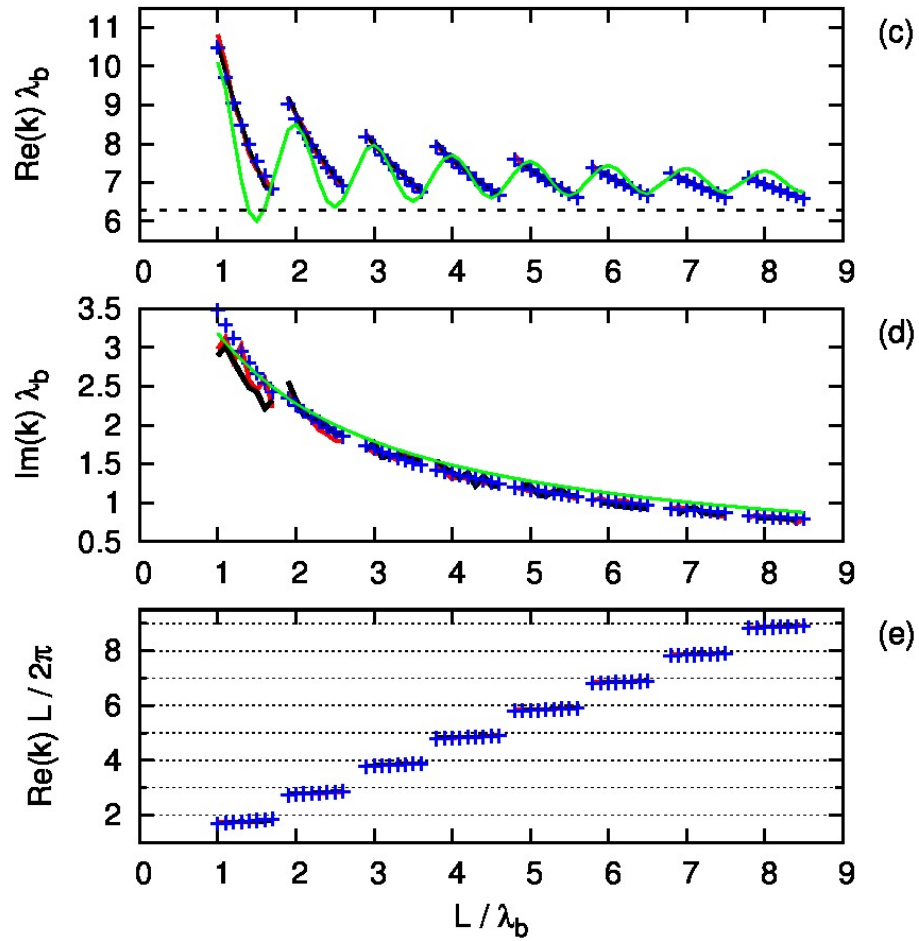

Frequency (a), temporal growth rate (b), wavenumber (c), spatial growth rate (d), and the number of wave periods per system length (e) versus the length of the system.
The blue crosses mark values obtained by analytical solution.

Solid red and black curves represent values obtained in fluid simulations with α = 0.00015 (red) and 0.0006 (black). Solid green curves are values provided by fitting formulas. In (c), the black dashed line marks the resonant wavenumber.

Summary of analytic model

We have studied the development of the two-stream instability in a finite size plasma bounded by electrodes both analytically and making use of fluid and particle-in-cell simulations.

We show that the instability reaches the asymptotic state when the wave structure has the same spatial profile and grows in time with a constant growth rate.

The spatial structure of the wave is close to a standing wave but has a spatial growth along the beam propagation.

We derived analytic expressions for the frequency, wave number and the spatial and temporal growth rates. Obtained analytic solution agrees well with the values given by fluid and particle-in-cell simulations.

- **Instability parameters are very different from the classical ones:**

growth rate $Im(\omega) \approx \frac{1}{13} L_n \ln(L_n) \left[1 - 0.18\cos\left(L_n + \frac{\pi}{2}\right)\right] \alpha\omega_{pe},$

where $L_n = L\omega_{pe}/v_b$, wavenumber $Re(k) \approx \frac{\omega_{pe}}{v_b}\left[1.1 + \frac{1+2.5\cos(L_n)}{1.1L_n}\right]$.

- **For comparison, the classical values:**

growth rate $Im(\omega) = 0.7\alpha^{1/3}\omega_{pe}$,

real resonance wavenumber $k = \omega_{pe}/v_b$.

OUTLINE

- **Beam-plasma interaction in a bounded plasma (two-stream instability):**

  - **Effects of nonuniform plasma**
    - **Density gradient plays a very important role in wave transformation and acceleration of bulk electrons.**
    - **It allows to couple the 800 eV beam and the bulk electrons with 2 eV temperature. =>**
  - **Mechanism of electron acceleration in plasma wave**

PRINCETON PLASMA PHYSICS LABORATORY

Short-wavelength plasma waves appear in the density gradient region

Initial profiles of electron density (top) and electrostatic potential (bottom).

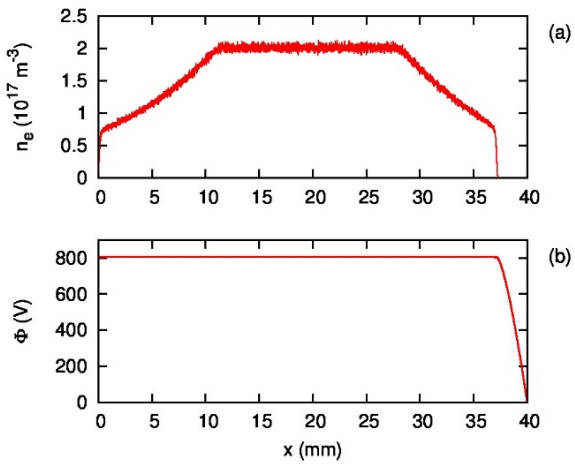

Cathode electron emission current 6.72 mA/cm2, relative beam density 0.000125.

Electric field vs coordinate (horizontal) and time (vertical).

Profile of the electric field at time marked by the arrow in the figure above. The anode is at x=0.

Amplitude of frequency spectrum of the electric field (color) vs the frequency (vertical axis) and coordinate (horizontal axis).

Electron plasma frequency (red) vs coordinate. The blue line marks the frequency excited by the beam.

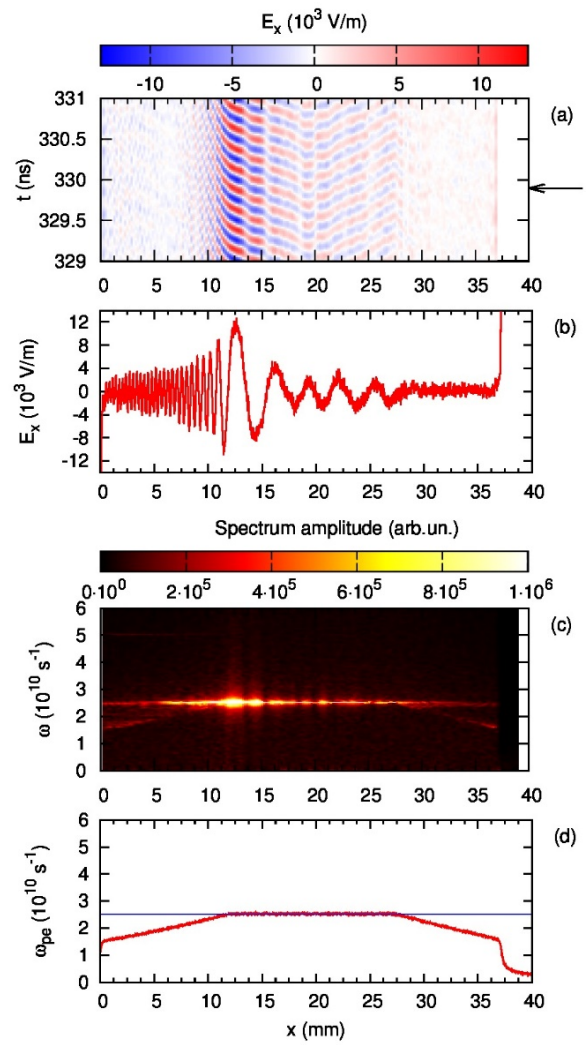

Mechanism of short-wavelength electron plasma wave excitation

Spectrum in k and w obtained for the electric field calculated in the simulation.

Theoretical dispersion: plasma wave in the density plateau (curve 1), plasma wave for density at x=5.9 mm (curve 2), the beam mode (curve 3), and the frequency excited by the beam (line 4).

$$\omega^2 = \omega_{pe}^2 + 3k^2 T_e/m_e$$

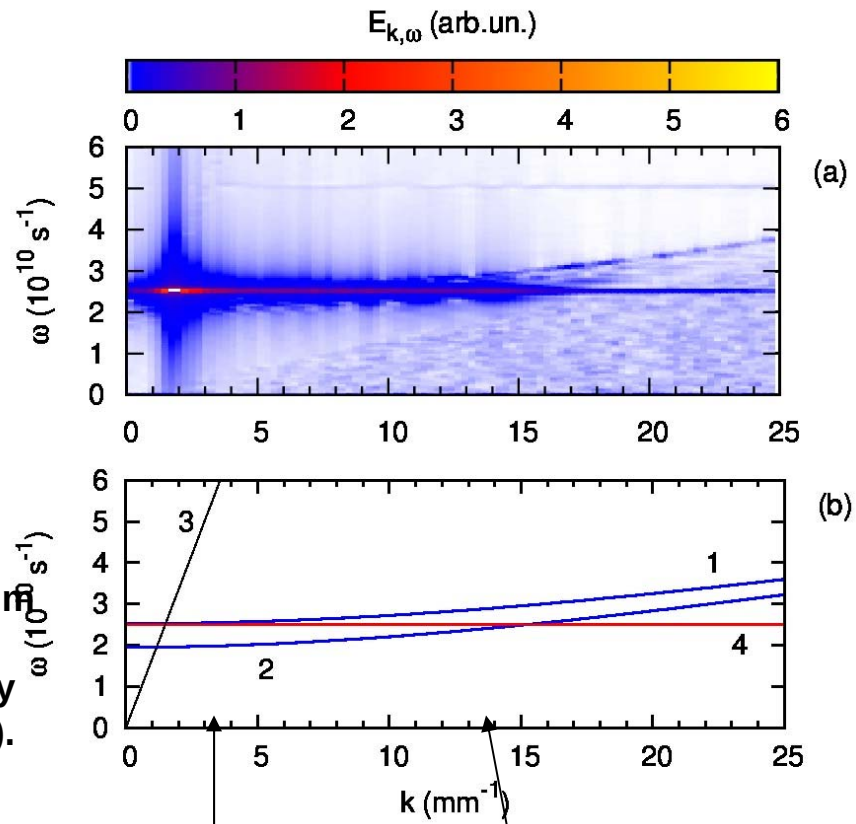

Wavenumber in the plateau area

Wavenumber in the density gradient area

The beam excites a strong plasma wave in the middle of the plasma.

The frequency of this wave defines the frequency of oscillations everywhere else.

In areas where the plasma density is lower, the wavenumber is larger, that is the wavelength is shorter.

Suprathermal electrons appear in simulation with higher beam current

The electron emission current at the cathode is 20.13 mA/cm^2, relative beam density is 0.000377.

Electric field amplitude vs time at x=12 mm (a) and vs coordinate and time (b)

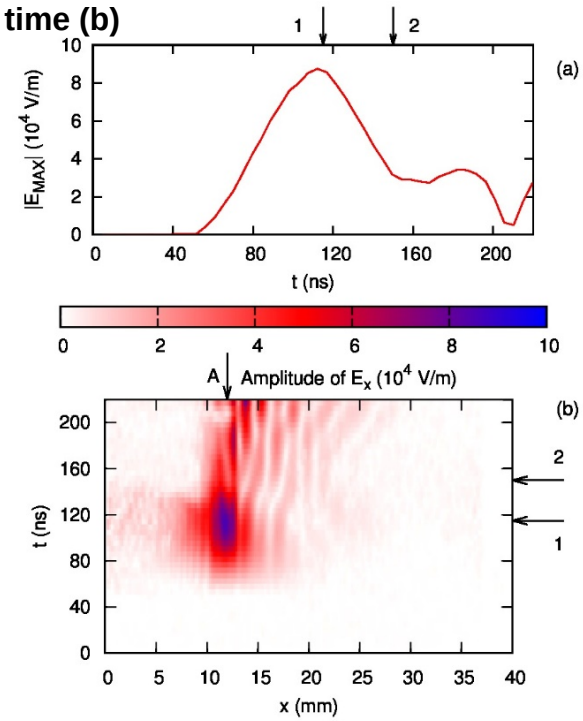

Electric field profile (a), phase plane v(x) (b), EVDF near anode (c). Time is 112 ns (left column, arrows 1) and 150 ns (right column, arrows 2).

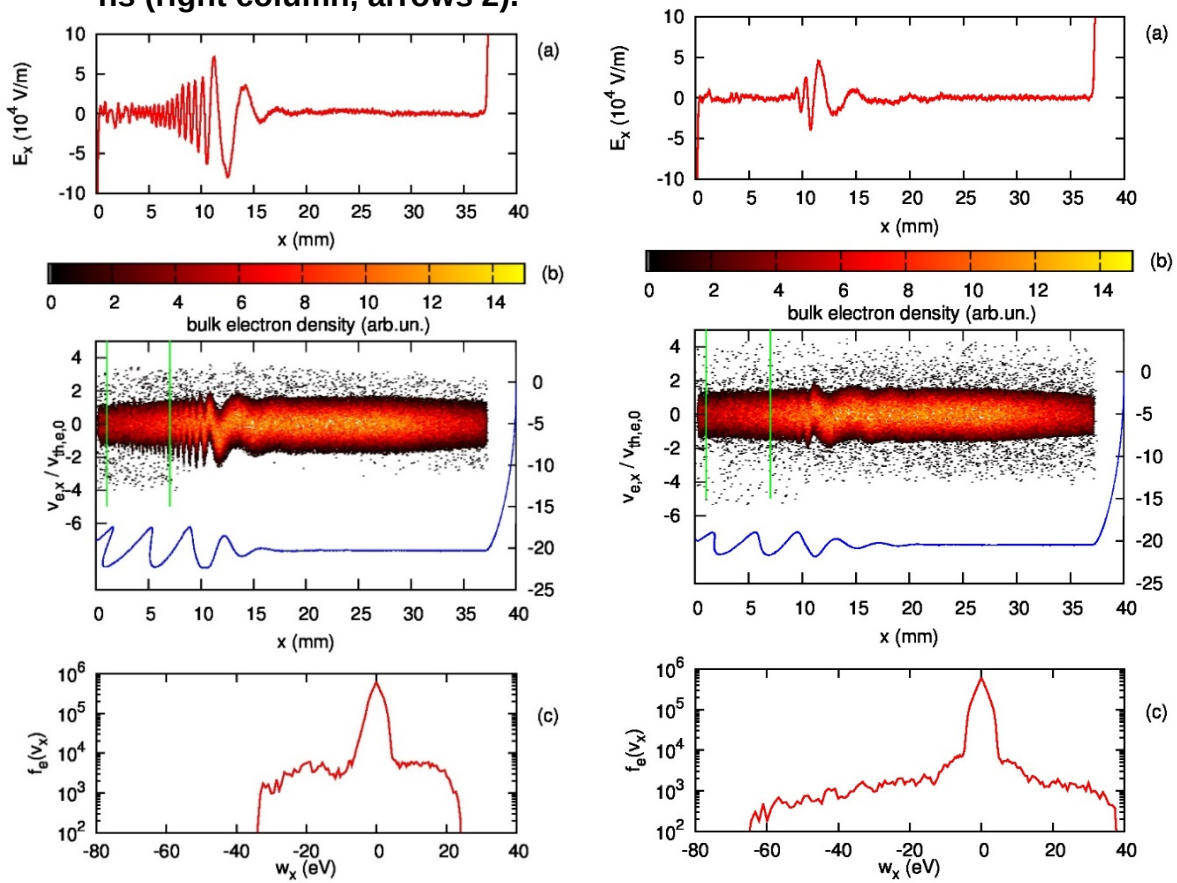

The energy of suprathermal electrons is significantly higher at later stage of instability when the wave amplitude is lower. Why?

Acceleration was studied with test particles

A representative profile of the electric field (top) and set of trajectories of test particles in the energy-coordinate phase space (bottom).

7 eV initial energy. Intense one-time acceleration.

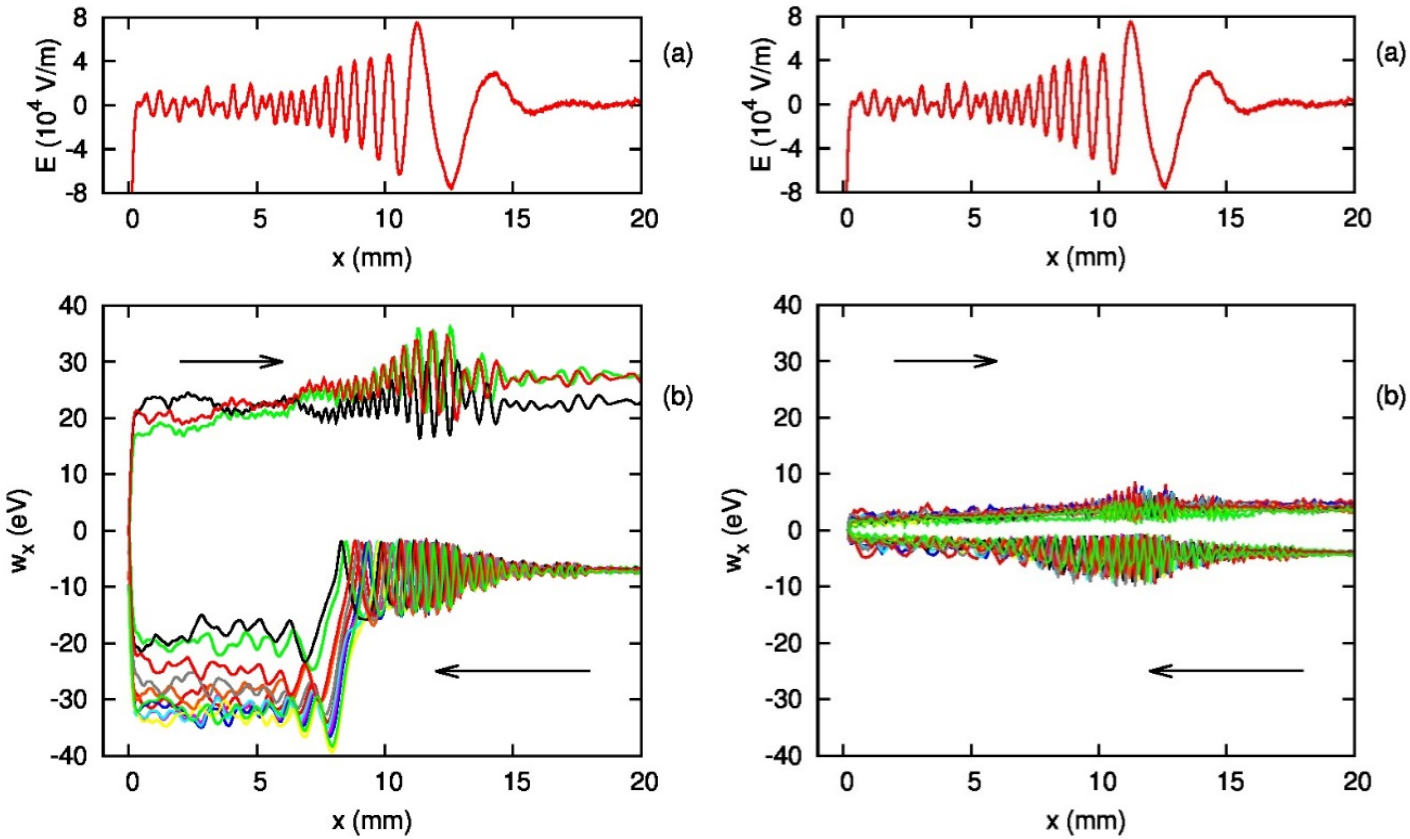

4 eV initial energy. No acceleration on average.

Acceleration is the combination of short resonance, strong field, and non-uniform wave phase velocity and amplitude

Color map of the electric field vs coordinate (horizontal axis) and time (vertical axis).

Phase space energy-coordinate.

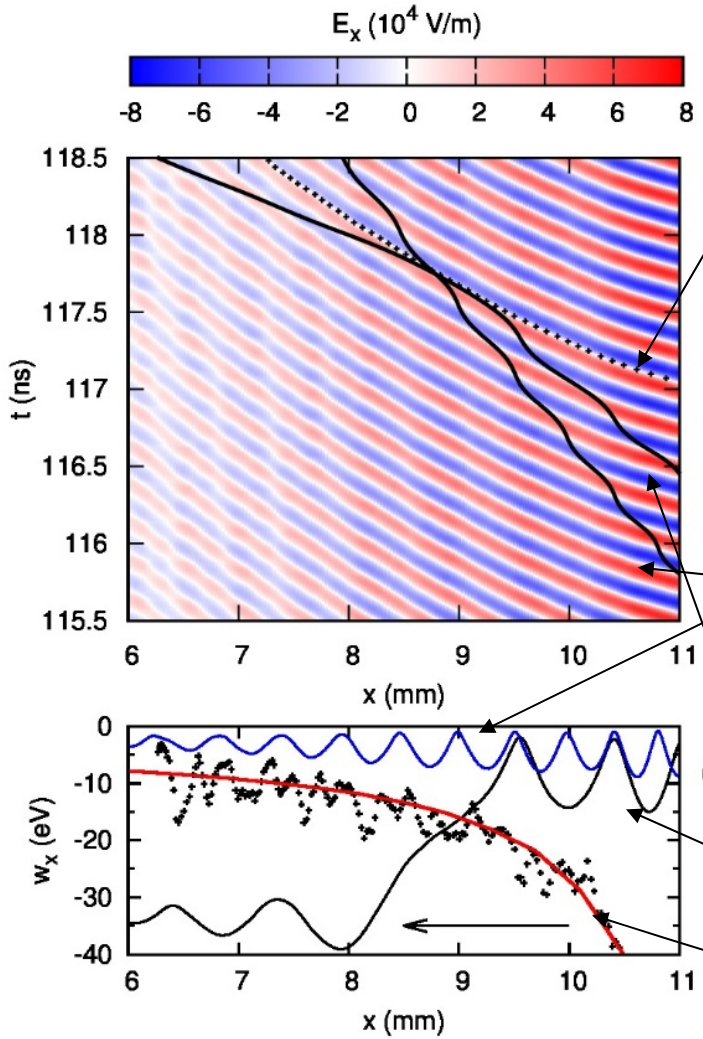

Phase speed of plasma wave calculated by differentiation of level lines (black markers) and theoretically (red curve).

$$\frac{\omega}{k} = \frac{\sqrt{3T_e/m_e}}{\sqrt{1-n(x)/n_0}}, \quad n_0 - n(x) >> n_0 \frac{3T_e}{2w_b}$$

Particle with initial energy 4 eV. No acceleration.

Particle with initial energy 7 eV.

The highest energy is acquired by recycled electrons

Color map of the electric field vs coordinate (horizontal axis) and time (vertical axis). Initial particle energy 6 eV.

First stage of acceleration.

Second stage of acceleration.

Phase space energy-coordinate.

O is the origin point, A is the first acceleration, B is the second acceleration, E – escape.

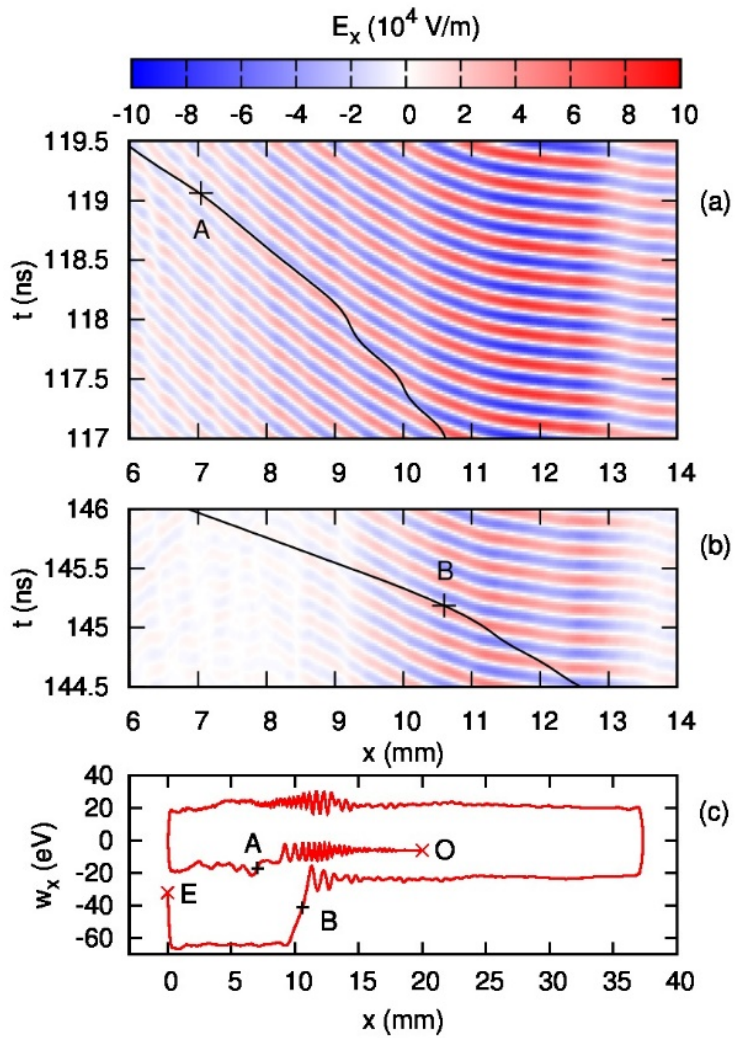

- Some electrons do not escape after the first acceleration.
- Such electrons make a round trip through the plasma and density gradient area with higher initial energy.
- They interact with the short waves in areas where the wave phase speed is higher, closer to the instability area.
- The energy after the second acceleration (~65eV) is an order of magnitude higher then the initial energy (~6eV).
- Such a mechanism explains why the highest energy suprathermal electrons appear with a delay.

The amplitude of instability grows with the beam current faster then expected

A set of simulations with beam current from 6.71 mA/cm^2 ($\alpha = 0.000125$) to 40.26 mA/cm^2 ($\alpha = 0.000755$) is performed.
The two-stage acceleration does not appear for $\alpha = 0.000125$ and $\alpha = 0.00019$.
With the two-stage acceleration, the maxmal energy of suprathermal electrons is much higher than that after the one-stage acceleration.

Markers are values from simulations.

Maximal electric field amplitude

Maximal potential perturbation amplitude

Maximal energy of suprathermal electrons

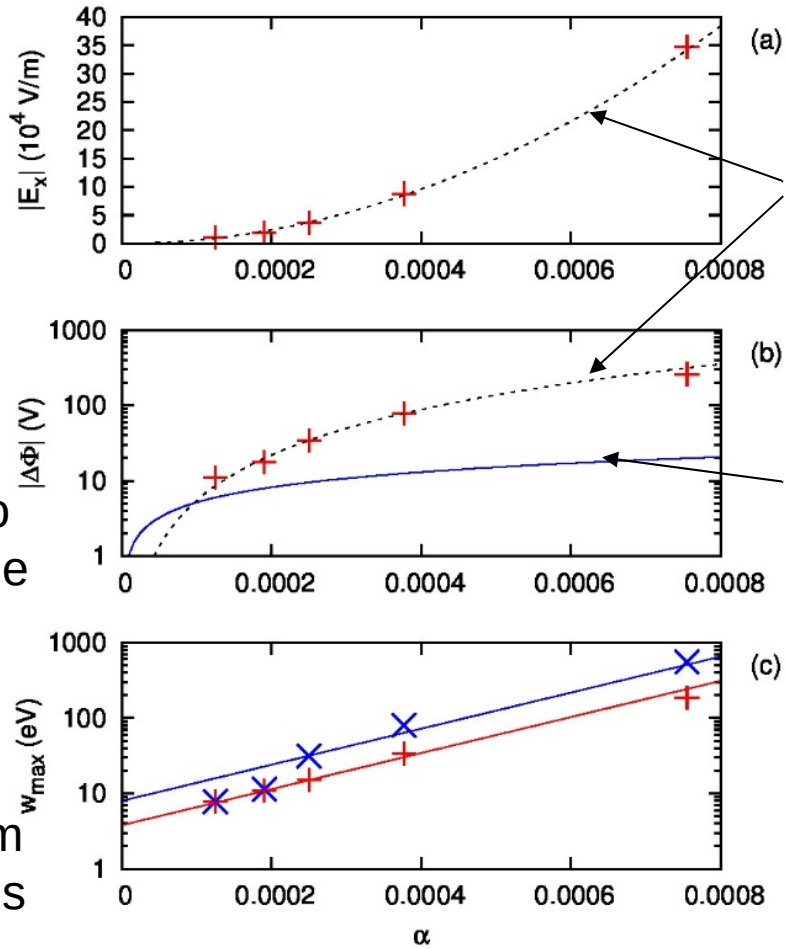

Relative density of the beam

Interpolation curves proportional to α^2

Saturation amplitude in an infinite plasma $e\Phi_{1,max} = 3w_b\alpha^{2/3}$

Red/blue crosses represent values before/after the two-stage acceleration.

Summary

- **We considered numerically the two-stream instability in a dc discharge with constant electron emission from a cathode.**
- **Plasma waves with short wavelength appear when a plasma wave excited by the beam enters a density gradient region with lower plasma density.**
- **The short-wavelength waves accelerate bulk electrons to suprathermal energies (from few eV to few tens of eV). Such acceleration is a one-time process and occurs along the direction of the wave phase speed decrease. It is possible because the wave phase speed and amplitude are strongly nonuniform.**
- **Some of the accelerated electrons may be reflected by the anode sheath and reintroduced into the density gradient area where they will be accelerated one more time. The energy of an electron after the second acceleration can be an order of magnitude higher than its initial energy.**
- **These processes may be relevant to observations of suprathermal (~100eV) peaks on the EVDF in a DC/RF discharge [Chen and Funk, 2010].**
- **The temporal growth rate and the amplitude of saturation of the instability are different functions of the beam density compared to the classical values obtained for infinite plasmas.**

Intermittency, ion waves, oscillations at the edges of the plasma

Electric field vs time in probe A

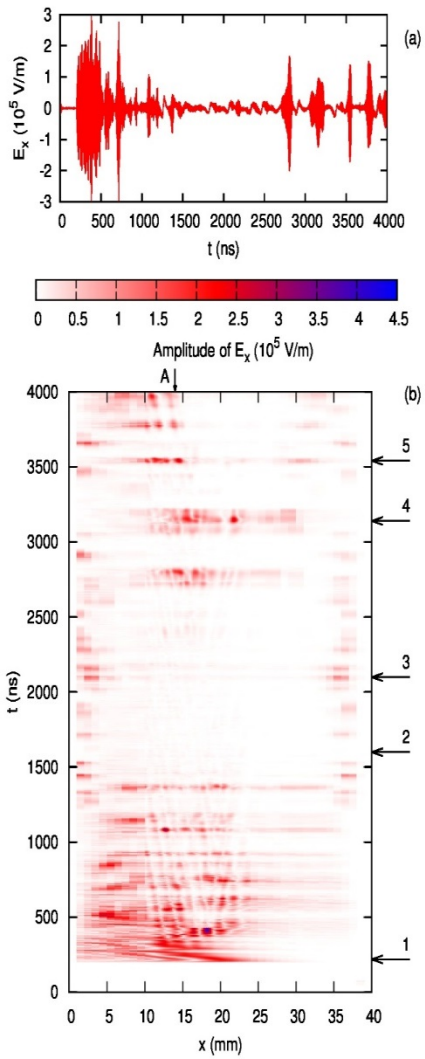

Amplitude of hf plasma oscillations vs coordinate (horizontal axis) and time (vertical axis)

Emission current 80.32 mA/cm^2, relative beam density 0.0016 (calculated with the initial bulk plasma density of 2×10^{11} cm^{-3}.)

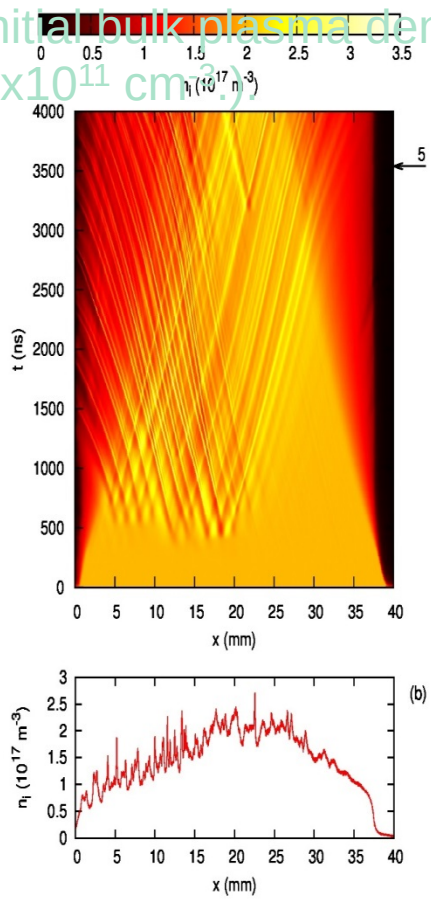

Ion density vs coordinate (horizontal axis) and time (vertical axis)

Ion density profile at time #5
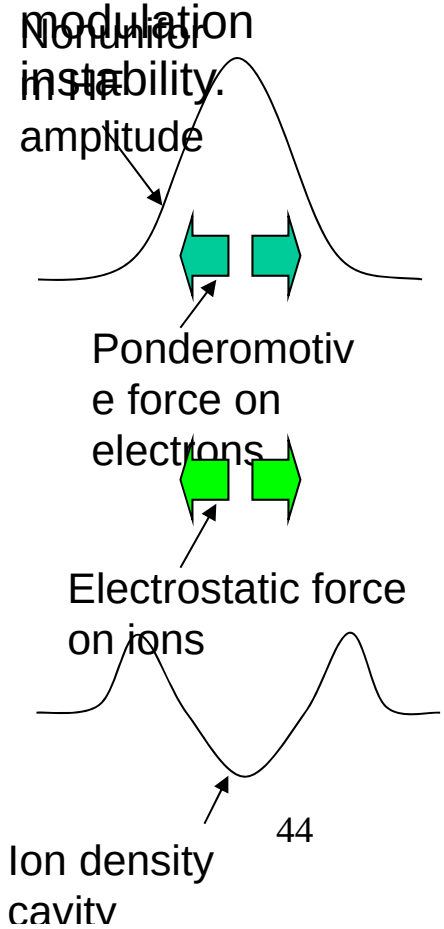
Ion waves are produced by intense HF fields due to the modulation instability.